Temperature and Salinity Dual-parameter Sensing Based on Forward Brillouin Scattering in 1060-XP SMF

LIU Pengkai[1,2], *ZHANG Wujun*[1,2], *LU Yuangang*[1,2*]

1. Key Laboratory of Space Photoelectric Detection and Perception of Ministry of Industry and Information Technology, Nanjing 211106, P. R. China;

2. College of Astronautics, Nanjing University of Aeronautics and Astronautics, Nanjing 211106, P. R. China

(Received 27 May 2024; revised 27 June 2024; accepted 14 July 2024)

Abstract: A novel temperature and salinity discriminative sensing method based on forward Brillouin scattering (FBS) in 1060-XP single-mode fiber (SMF) is proposed. The measured frequency shifts corresponding to different radial acoustic modes in 1060-XP SMF show different sensitivities to temperature and salinity. Based on the new phenomenon that different radial acoustic modes have different frequency shift-temperature and frequency shift-salinity coefficients, we propose a novel method for simultaneously measuring temperature and salinity by measuring the frequency shift changes of two FBS scattering peaks. In a proof-of-concept experiment, the temperature and salinity measurement errors are 0.12 ℃ and 0.29%, respectively. The proposed method for simultaneously measuring temperature and salinity has the potential applications such as ocean surveying, food manufacturing and pharmaceutical engineering.

Key words: forward Brillouin scattering(FBS); optical fiber sensor; salinity sensing; temperature sensing

CLC number: TP212.1 **Document code:** A **Article ID:** 1005-1120(2024)S-0089-07

0 Introduction

Simultaneous measurement of temperature and salinity is crucial for many applications in food industry, pharmaceutical engineering and chemical industry[1-2]. So far, the methods for measuring salinity require complex process processing or low mechanical strength[3]. The acoustic vibration involved in forward Brillouin scattering (FBS) is a transverse acoustic field[4]. In the reported optical fiber sensors based on FBS, only single and dual parameter simultaneous measurement methods for temperature and acoustic impedance sensing can be achieved[5-12]. Until now, no researchers have used FBS to measure temperature and salinity simultaneously. However, other commonly used sensing fibers such as G655 single-mode fiber (SMF)[6] have lower sensitivity to salinity. In order to obtain a temperature and salinity simultaneous measurement sensor with small size, light weight, and corrosion resistance, we propose a new temperature and salinity discriminative sensing based on FBS in 1060-XP SMF.

In this work, we firstly present new findings that the frequency shift dependencies of radial acoustic modes induced FBS spectrum on temperature and salinity are different with different acoustic modes in 1060-XP fiber. Based on the new findings, we propose a novel dual-parameter sensing method capable of simultaneously measuring temperature and salinity with high mechanical strength.

1 Sensing Principle

The frequency shift ν_m of the resonance peak of the FBS spectra induced by the radial acoustic mode $R_{0,m}$ (The m is order number) in an ideal cylindrical optical fiber is defined by[13]

*Corresponding author, E-mail address: luyg@nuaa.edu.cn.

How to cite this article: LIU Pengkai, ZHANG Wujun, LU Yuangang. Temperature and salinity dual-parameter sensing based on forward Brillouin scattering in 1060-XP SMF[J]. Transactions of Nanjing University of Aeronautics and Astronautics, 2024, 41(S): 89-95.

http://dx.doi.org/10.16356/j.1005-1120.2024.S.011

$$\nu_m = \frac{y_m \cdot \nu_L}{2\pi a} \tag{1}$$

where a is the radius of fiber outer, y_m the eigenvalue of $R_{0,m}$ acoustic modes, and ν_L the velocity of the longitudinal acoustic wave.

When the salinity of the solution around the optical fiber changes, it will cause a change in the liquid density and sound velocity of the fiber surrounding environment which in turn leads to a change in the acoustic impedance of the environment[14]. Due to the approximate linear relationship between y_m and the acoustic impedance Z of medium surrounding the fiber, the value will also change with the change of the acoustic impedance of the surrounding solution, which can be expressed as $y_m \sim Z$[15-17]. According to Eq.(1), as y_m changes, the frequency shift of the FBS spectrum induced by $R_{0,m}$ acoustic modes changes which can be expressed as $v_m \sim Z$[5-7]. Therefore, if the salinity S is linearly related with Z, the frequency shift of FBS spectrum can be used to detect salinity.

It is known that the frequency shift of FBS changes linearly with the temperature[6,10]. Then, if there is a linear relationship between the frequency shift of FBS and salinity surrounding a sensing fiber, a novel temperature and salinity discriminative sensing method based on FBS can be realized. The frequency shifts of $R_{0,i}$ and $R_{0,j}$ (i and j are the order numbers of $R_{0,m}$, $i \neq j$) induced FBS spectrum are denoted as ν_i and ν_j, respectively, which can be expressed as

$$\nu_i = \nu_{i\_0} + C_{\nu T\_i} \cdot \Delta T + C_{\nu S\_i} \cdot \Delta S \tag{2}$$

$$\nu_j = \nu_{j\_0} + C_{\nu T\_j} \cdot \Delta T + C_{\nu S\_j} \cdot \Delta S \tag{3}$$

where ν_{i_0} and ν_{j_0} are the frequency shifts of $R_{0,i}$ and $R_{0,j}$ induced FBS spectrum at original state, respectively. $C_{\nu T\_i}$ and $C_{\nu T\_j}$ are the frequency shift-temperature coefficients corresponding to $R_{0,i}$ and $R_{0,j}$, respectively. $C_{\nu S\_i}$ and $C_{\nu S\_j}$ are the frequency shift-salinity coefficients corresponding to $R_{0,i}$ and $R_{0,j}$ acoustic modes, respectively. ΔT and ΔS correspond to the changes of temperature and salinity, which can be obtained from Eqs.(2, 3), and can be expressed as

$$\begin{bmatrix} \Delta T \\ \Delta S \end{bmatrix} = \begin{bmatrix} C_{\nu T\_i} & C_{\nu S\_i} \\ C_{\nu T\_j} & C_{\nu S\_j} \end{bmatrix}^{-1} \begin{bmatrix} \Delta \nu_i \\ \Delta \nu_j \end{bmatrix} \tag{4}$$

where $\Delta\nu_i$ and $\Delta\nu_j$ are the changes of the frequency shifts of the FBS spectrum induced by $R_{0,i}$ and $R_{0,j}$, respectively. Therefore, by calculating Eq.(4), a novel method to achieve temperature and salinity simultaneous measurement by using the frequency shift information of two $R_{0,m}$ acoustic modes is proposed. It should be noted that, in order to achieve this new dual-parameter sensing method, one must find sensing fibers that meet the linear relationship in Eq.(4). We will select 1060-XP as a new type of sensing fiber that meets this linear relationship through experiments in the next section.

The measurement errors of the frequency shifts of $R_{0,i}$ and $R_{0,j}$ induced FBS spectrum ($\delta\nu_i$ and $\delta\nu_j$) can be expressed as follows

$$\delta\nu_i = C_{\nu T\_i} \cdot \delta T + C_{\nu S\_i} \cdot \delta S \tag{5}$$

$$\delta\nu_j = C_{\nu T\_j} \cdot \delta T + C_{\nu S\_j} \cdot \delta S \tag{6}$$

where δT and δS are the temperature and salinity measurement errors, respectively. By using the frequency shift information of $R_{0,i}$ and $R_{0,j}$ induced FBS spectrum for temperature and salinity simultaneous measurement, the temperature and salinity measurement errors can be expressed as follows

$$\begin{bmatrix} \delta T \\ \delta S \end{bmatrix} = \begin{bmatrix} C_{\nu T\_i} & C_{\nu S\_i} \\ C_{\nu T\_j} & C_{\nu S\_j} \end{bmatrix}^{-1} \begin{bmatrix} \delta \nu_i \\ \delta \nu_j \end{bmatrix} \tag{7}$$

2 Experiment and Results

The schematic experimental setup of the proposed sensing system is shown in Fig.1. The laser source is a narrow-linewidth fiber laser (5 kHz) with a central wavelength of 1 550 nm. After passing through an optical isolator (ISO) and a polarization controller (PC), the output light with a power of 8.6 dBm is transmitted into a fiber Sagnac loop that consists of a 2 × 2 fiber coupler, a PC and the fiber under test (FUT). In order to achieve a good signal-to-noise ratio and use suitable optical fiber with appropriate length, we chose a 30 m long 1060-XP fiber as the FUT. The diameters of cladding and core of the 1060-XP fiber used in the experiment are 125 μm and 5.3 μm, respectively[18-19]. The ISO protects the laser from damage induced by light reflection back to the laser. In the FUT, the $R_{0,m}$ acoustic modes are excited, which apply phase modulation

to the propagating light[7-9,20]. By adjusting the PC, the torsional-radial acoustic mode can be suppressed as much as possible to reduce its influence on the $R_{0,m}$ acoustic mode[13,21]. The fiber Sagnac loop converts the phase modulation into the intensity modulation[7-8]. Then the intensity-modulation signal is detected by a photodetector (PD) with 1.6 GHz bandwidth and the FBS spectrum is monitored by an electrical spectrum analyzer (ESA)[5].

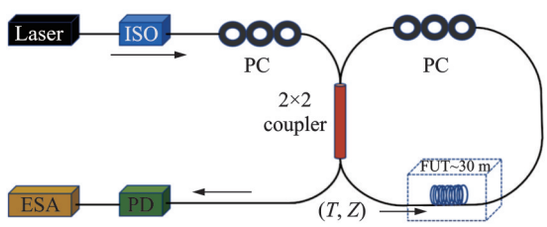

Fig.1 Schematic diagram of the experimental setup for observing FBS spectrum

The measured FBS spectrum of FUT at room temperature is shown in Fig.2. In addition, the resonance peaks of the adjacent FBS spectrum induced by $R_{0,m}$ acoustic modes have similar frequency intervals (around 48 MHz)[22].

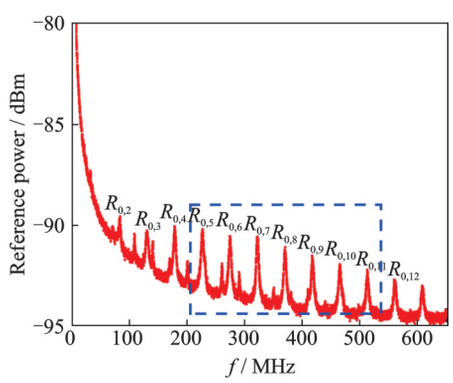

Fig.2 The measured FBS spectrum of FUT in distilled water at room temperature

First, the FUT is placed in a heating plate, and the frequency shifts of the FBS resonance peaks with the change of temperature are measured. The temperature is changed from 22 ℃ to 50 ℃ with a step of 4 ℃. The frequency resolution bandwidth (RBW) and video resolution bandwidth (VBW) of ESA are set to 50 and 5 kHz, respectively. The FBS spectrum is averaged 1 000 times. The frequency shift-temperature coefficients ($C_{\nu T}$) for $R_{0,5}$ to $R_{0,11}$ is shown in Fig.3(a). We find that for the 1060-XP fiber, the frequency shifts of the FBS induced by $R_{0,m}$ acoustic modes have linear relationships with temperature in this temperature range.

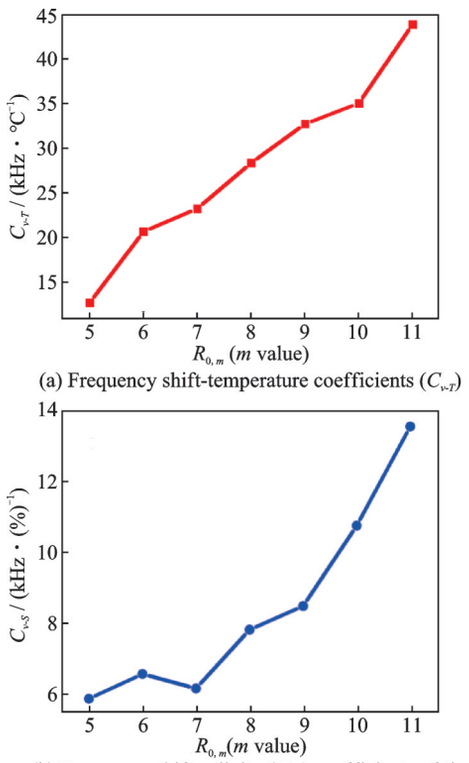

Fig.3 The measured frequency shift-temperature coefficients ($C_{\nu T}$) and frequency shift-salinity coefficients ($C_{\nu S}$) of the FBS spectrum induced by $R_{0,5}$ to $R_{0,11}$ in FUT

Next, the FUT is placed in NaCl solution and the frequency shifts of the FBS resonance peaks with the change of salinity are measured. The environment temperature is set to room temperature (22 ℃), and the salinity of saline water is changed from 0 to 15% with a step of 3%. The frequency shift-salinity coefficient ($C_{\nu S}$) for $R_{0,5}$ to $R_{0,11}$ is shown in Fig.3(b). The frequency RBW of ESA is set to 5 kHz and the FBS spectrum is averaged 1 000 times. In the range of 0 to 15%, the frequency shift of FBS of the 1060-XP fiber increases with the increase of salinity, and there is a linear relationship between frequency shift and salinity at different $R_{0,m}$ acoustic modes. It can be found that higher-order acoustic modes have higher temperature and sa-

linity sensitivities.

As shown in Eq.(4), two different modes can be chosen to realize the temperature and salinity discriminative sensing. To get the best measurement errors, we need to use Eq.(7) and the coefficients in Fig.3 to find the optimal portfolio ($R_{0,i}$, $R_{0,j}$) ($5 \leqslant i, j \leqslant 11$, $i \neq j$) that gives the lowest temperature and salinity measurement errors. In the experiment, to obtain $\delta\nu_i$ and $\delta\nu_j$ in Eq.(7), the frequency shift corresponding to each $R_{0,m}$ acoustic mode is measured for 7 times, and the standard deviation of the frequency shift is calculated. The values of $\delta\nu_5$, $\delta\nu_6$, $\delta\nu_7$, $\delta\nu_8$, $\delta\nu_9$, $\delta\nu_{10}$ and $\delta\nu_{11}$ are 2.5, 6.8, 2.3, 6.4, 6.5, 7 and 6.9 kHz, respectively. Taking the temperature repeatability measurement as an example, the deviation of the temperature measured within 1 min is about 0.1 ℃. It indicates that the sensing system and the FBS spectra we obtained both have good stabilities. We obtain the calculation measurement results for the temperature and salinity in Fig.4. For all the sets of ($R_{0,i}$, $R_{0,j}$) ($5 \leqslant i, j \leqslant 11$, $i \neq j$), the set ($R_{0,5}$, $R_{0,11}$) has the lowest measurement errors, which are 0.08 ℃ and 0.26%, respectively.

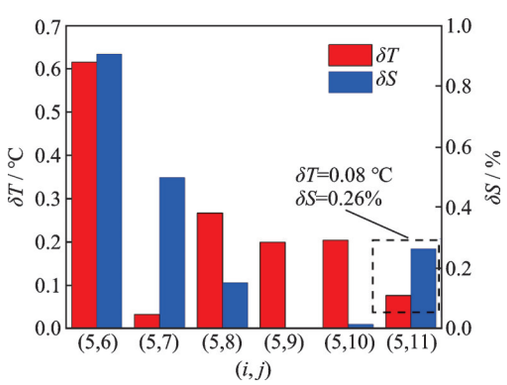

Fig.4 The temperature and salinity measurement errors of the sets of ($R_{0,i}$, $R_{0,j}$) ($i=5$, $6 \leqslant j \leqslant 9$)

Based on the above calculation results, we selected $R_{0,5}$ and $R_{0,11}$ for the temperature and salinity discriminative sensing. As shown in Figs.5(a,b), the temperature and salinity sensitivities of $R_{0,5}$ ($C_{\nu\text{-}T,5}$ and $C_{\nu\text{-}S,5}$) are 12.68 kHz/℃and 5.85 kHz/%, respectively, the temperature and salinity sensitivities of $R_{0,11}$ ($C_{\nu\text{-}T,11}$ and $C_{\nu\text{-}S,11}$) are 44.01 kHz/℃ and 13.54 kHz/%, respectively.

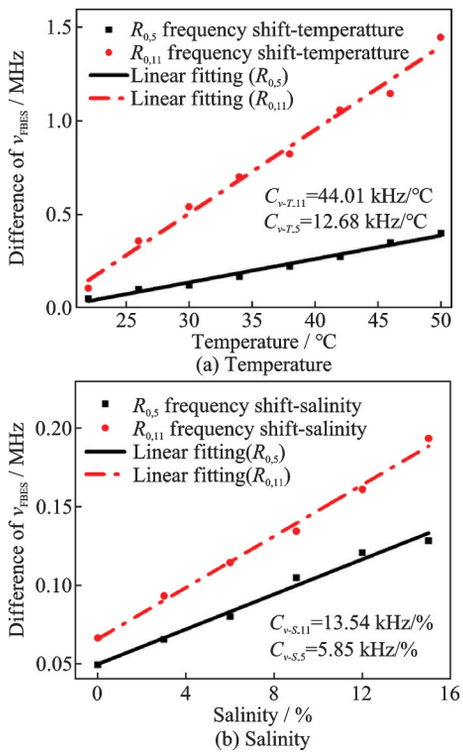

Fig.5 The measured frequency shift of the FBS scattering peaks induced by $R_{0,5}$ and $R_{0,11}$ acoustic modes as a function of temperature and salinity

In order to more conveniently verify the measured results with the calculated results, 45 ℃ distilled water (0% NaCl solution in water) is selected as State 1. Then the 10% NaCl solution in water at the temperature of 26 ℃ is selected as State 2. The actual temperatures of two states are controlled close to 45 ℃ and 26 ℃, which are 45.68 ℃ and 26.76 ℃, respectively. Figs.6(a,b) show the measured FBS spectrum induced by $R_{0,5}$ acoustic mode at State 1 and State 2, respectively, where the corresponding measured central frequencies (ν_{5_1} and ν_{5_2}) are 226.659 MHz and 226.840 MHz, respectively. The measured FBS spectrum induced by $R_{0,11}$ acoustic mode at State 1 and State 2 are shown in Figs.6(c,d), respectively, where the corresponding measured central frequencies (ν_{11_1} and ν_{11_2}) are 513.720 MHz and 514.416 MHz, respectively.

The temperature decreases by 18.92 ℃ and the salinity increases by 10%, that is, ΔT is −18.92 ℃ and ΔS is 10%. Substituting the corresponding center frequencies of the two states into Eqs.(2—4), the measured temperature change $\Delta T'$ and salinity change $\Delta S'$ are −18.80 ℃ and 9.81%, respectively.

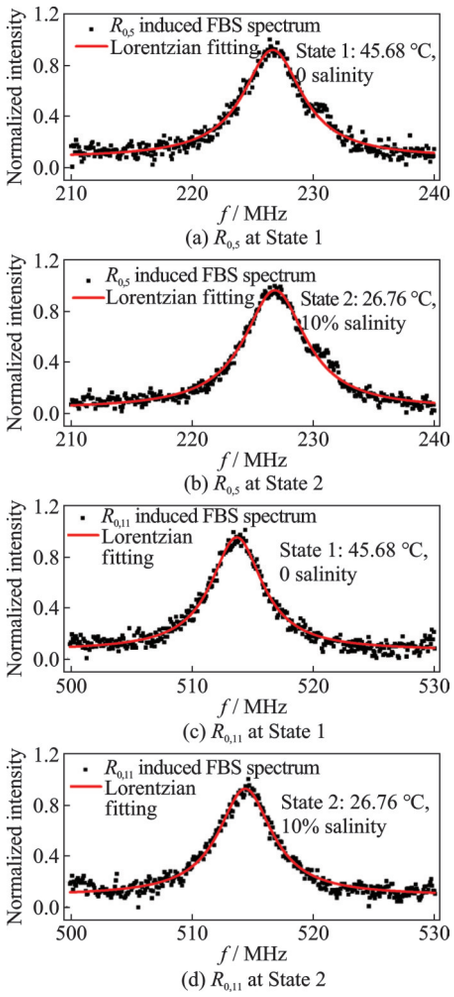

Fig.6 The measured FBS spectrum induced by radial acoustic modes of $R_{0,5}$ at State 1 and State 2, and $R_{0,11}$ at State 1 and State 2

Therefore, the measurement errors of temperature and salinity are 0.12 ℃ and 0.29%, respectively, which are in good agreement with the theoretical error values of 0.08 ℃ and 0.26%. The differences between experimental results and theoretical results may originate from the evaluated errors of linear coefficients and the temperature fluctuation of the temperature control system.

In our two parameter measurement environment, the frequency shift of FBS is only sensitive to the three measured parameters. As shown in Eqs.(2—4), it is precisely because there are no other parameters in the measurement environment that in the frequency shifts change, taking into account the cross-sensitivity characteristics of these two measured environment parameters. Therefore, the sensing system has good repeatability.

The sensing performance of the proposed sensor by using 1060-XP fiber is compared with other optical fiber sensors, as shown in Table 1. It is found that the proposed method has a high sensitivity, a low measurement error with great mechanical strength. In the future, utilizing the correlation between the linewidth of the forward Brillouin scattering peak and parameters such as temperature and pressure, it can also be achieved to simultaneously measure three parameters using three different linewidths of $R_{0,m}$ acoustic modes[25-26].

Table 1 Perpormance evaluation for different sensors

Ref.	Type	Temperature measurement error/℃	Salinity measurement error/%	Mechanical strength
[23]	FBS	0.65	—	High
[24]	OFDR	1.20	—	Medium
[6]	FBS	0.10	0.18	Low
[7]	FBS	—	2.03	High
This work	FBS	0.12	0.29	High

3 Conclusions

The temperature and salinity characteristics of $R_{0,m}$ acoustic modes induced FBS in 1060-XP optical fibers and their dependence on temperature and salinity are experimentally demonstrated. Then a method for simultaneous measurement of temperature and salinity using FBS is proposed and experimentally validated. The obtained measurement errors of temperature and salinity are 0.12 ℃ and 0.29%, respectively, with high measurement errors. The proposed method for simultaneous measurement of temperature and salinity has great potential applications in food industry, pharmaceutical engineering and chemical industry.

References

[1] LIEBERMAN R A, BLYLER L L, COHEN L G. A distributed fiber optic sensor based on cladding fluorescence[J]. Journal of Lightwave Technology, 1990, 8(2): 212-220.

[2] KATO Y, WADA Y, MIZUNO Y, et al. Measurement of elastic wave propagation velocity near tissue surface by optical coherence tomography and laser Doppler velocimetry[J]. Japanese Journal of Applied Physics, 2014, 53(7): 07KF05.

[3] QIAN Y, ZHAO Y, WU Q, et al. Review of salinity measurement technology based on optical fiber sensor[J]. Sensors and Actuators, B: Chemical, 2018, 260: 86-105.

[4] STEPANOV D Y, COWLE G J. Properties of Brillouin/Erbium fiber lasers[J]. IEEE Journal of Selected Topics in Quantum Electronics, 1997, 3(4): 1049-1057.

[5] ZHANG Z, LU Y, TANAKA Y, et al. Discriminative sensing of temperature and acoustic impedance by using forward Brillouin scattering in large effective area fiber[J]. Applied Physics Express, 2021, 14(4): 042004.

[6] ZHANG Z, LU Y, PENG J, et al. Simultaneous measurement of temperature and acoustic impedance based on forward Brillouin scattering in LEAF[J]. Optics Letters, 2021, 46(7): 1776-1779.

[7] CHOW D M, THÉVENAZ L. Forward Brillouin scattering acoustic impedance sensor using thin polyimide-coated fiber[J]. Optics Letters, 2018, 43(21): 5467-5470.

[8] ZHENG Z, LI Z, FU X, et al. Multipoint acoustic impedance sensing based on frequency-division multiplexed forward stimulated Brillouin scattering[J]. Optics Letters, 2020, 45(16): 4523-4526.

[9] NISHIZAWA N, KUME S, MORI M, et al. Experimental analysis of guided acoustic wave Brillouin scattering in PANDA fibers[J]. Journal of the Optical Society of America B: Optical Physics, 1995, 12(9): 1651-1655.

[10] TANAKA Y, OGUSU K. Temperature coefficient of sideband frequencies produced by depolarized guided acoustic-wave Brillouin scattering[J]. IEEE Photonics Technology Letters, 1999, 10(12): 1769-1771.

[11] HENG X, GAN J, ZHANG Z, et al. Transverse mode switchable all-fiber Brillouin laser[J]. Optics Letter, 2018, 43(17): 4172-4175.

[12] LUO Y, TANG Y, YANG J, et al. High signal-to-noise ratio, single-frequency 2 μm Brillouin fiber laser[J]. Optics Letter, 2014, 39(9): 2626-2628.

[13] HAYASHI N, SUZUKI K, SET S Y, et al. Temperature coefficient of sideband frequency produced by polarized guided acoustic-wave Brillouin scattering in highly nonlinear fibers[J]. Applied Physics Express, 2017, 10(9): 092501.

[14] ANTMAN Y, CLAIN A, LONDON Y, et al. Optomechanical sensing of liquids outside standard fibers using forward stimulated Brillouin scattering[J]. Optica, 2016, 3(5): 510-516.

[15] PUTTMER A, HAUPTMANN P, HENNING B. Ultrasonic density sensor for liquids[J]. IEEE Transactions on Sonics and Ultrasonics, 2000, 47(1): 85-92.

[16] GRONAU G, WOLFF I. Application of Brillouin amplification in coherent optical transmission[J]. Electronics Letters, 1986, 22(10): 556-558.

[17] SHELBY R M, LEVENSON M D, BAYER P W, et al. Guided acoustic-wave Brillouin scattering[J]. Physical Review B, 1985, 31: 5244-5252.

[18] WANG Q, GERALD F, THOMAS F. Theoretical and experimental investigations of macro-bend losses for standard single mode fibers[J]. Optics Express, 2005, 13(12): 4476-4484.

[19] YANG C, YANG Z. Fusion splicing experiments of 1060-XP silica fiber with phosphate glass fiber[J]. Journal of Wuhan University of Technology (Materials Science Edition), 2007, 1: 847-849.

[20] CHOW D M, YANG Z, SOTO M A, et al. Distributed forward Brillouin sensor based on local light phase recovery[J]. Nature Communications, 2018, 9(1): 1-9.

[21] HUA Z, BA D, ZHOU D, et al. Non-destructive and distributed measurement of optical fiber diameter with nanometer resolution based on coherent forward stimulated Brillouin scattering[J]. Light: Advanced Manufacturing, 2021, 2(4): 373-384.

[22] SHIN H, QIU W, JARECKI R, et al. Tailorable stimulated Brillouin scattering in nanoscale silicon waveguides[J]. Nature Communications, 2013. DOI: 10.1038/ncomms2943.

[23] ANTMAN Y, LONDON Y, ZADOK A. Scanning-free characterization of temperature dependence of forward stimulated Brillouin scattering resonances[J]. Optical Fiber Sensors, 2015, 9634: 96345C.

[24] ZHOU D P, LI W, CHEN L, et al. Distributed temperature and strain discrimination with stimulated Brillouin scattering and Rayleigh backscatter in an optical fiber[J]. Sensors, 2013, 13(2): 1836-1845.

[25] DENG C, HOU S, LEI J, et al. Simultaneous measurement on strain and temperature via guided acoustic-wave Brillouin scattering in single mode fibers[J]. Acta Physica Sinica, 2016, 65(24): 240702.

[26] SANCHEZ L A, DIEZ A, CRUZ J L, et al. Strain and temperature measurement discrimination with forward Brillouin scattering in optical fibers[J]. Optics Express, 2022, 30(9): 14384-14392.

Acknowledgements This work was supported by the National Natural Science Foundation of China (Nos.62175105,

61875086), and Fundamental Research Funds for the Central Universities of China (No.ILB240041A24).

Authors Mr. **LIU Pengkai** received his M.S. degree from Nanjing University of Aeronautics and Astronautics, Nanjing, China, in 2024. His research focuses on forward Brillouin scattering fiber optic sensing technology.

Prof. **LU Yuangang** is currently a full professor of the College of Astronautics, Nanjing University of Aeronautics and Astronautics, Nanjing, China. His research interests include optical metrology, optical information processing, and optical fiber sensing.

Author contributions Mr. **LIU Pengkai** contributed to calculation and experiment, and wrote the manuscript. Prof. **LU Yuangang** designed and guided the study, and gave key opinions on the core issues. Ms. **ZHANG Wujun** conducted some related work about the experiment. All authors commented on the manuscript draft and approved the submission.

Competing interests The authors declare no competing interests.

(Production Editor: XU Chengting)

基于前向布里渊散射1060-XP单模光纤的温度和盐度双参量传感

刘鹏凯[1,2]，张伍军[1,2]，路元刚[1,2]

(1.空间光电探测与感知工业和信息化部重点实验室，南京 211106，中国；
2.南京航空航天大学航天学院，南京 211106，中国)

摘要：提出了一种新的基于前向布里渊散射(Forward Brillouin scattering, FBS)的1060-XP单模光纤(Single-mode fiber, SMF)温度和盐度判别传感方法。1060-XP单模光纤中不同径向声学模式的测量频移具有对温度和盐度的不同敏感度。基于不同径向声学模式具有不同频移温度和频移盐度系数，本文提出了一种通过测量两个FBS散射峰的频移变化来同时测量温度和盐度的新方法。在概念验证实验中，温度和盐度的测量误差分别为0.12 ℃和0.29‰。所提出的同时测量温度和盐度的方法在海洋测量、食品制造和制药工程等领域中具有潜在应用。

关键词：前向布里渊散射；光纤传感器；盐度传感；温度传感